Passive and active spectroscopy on flowing plasmas

High Temp. Chem. Processes 3 (1994) 601–612 DECEMBER **1994**, PAGE 601

Passive and active spectroscopy on flowing plasmas

J.A.M. van der Mullen, M.C.M. van de Sanden, B. van der Sijde and D.C. Schram

Eindhoven University of Technology, Faculty of Physics, P.O. Box 513, 5600 MB Eindhoven, The Netherlands

Abstract : The equilibrium departures of two types of flowing plasmas are studied experimentally. The combination of absolute emission spectroscopy with the non-intrusive active tool of Thomson/Rayleigh scattering makes it possible to compare the atomic state distribution function (ASDF) with its equilibrium form. The electron excitation kinetics (EEK) of a highly recombinative Cascaded Arc Created Magnetized Expanding Plasma is studied using time resolved laser induced fluorescence. The recombination process is found to be largely affected by heavy particle excitation kinetics (HEK). A comparable study of an inductively coupled plasma reveals that the deviations from partial local Saha equilibrium (pLSE) are much less pronounced. To get insight in this plasma, global active spectroscopy is performed by following the response to the power interruption.

A list of abbreviations is given at the end, just before the list of references

1. INTRODUCTION

The definition of a thermal plasma as an electrically conducting gas with electrons and heavy particles in thermal equilibrium suggests that the diagnostics of such a medium is simple. Apart from the pressure and chemical composition only the value of one extra parameter e.g. the temperature, needs to be known. Other quantities can be derived from this temperature using the equation of state. The fact that so many publications are devoted to the diagnostics of thermal plasmas proves that the actual situation is not as simple as suggested by the definition quoted above.

In treating this contradiction we divide plasmas into ionizing and recombining regions. In the ionizing zone the plasma creation takes place due to excitation and ionization processes executed by electrons accelerated in the electric field. The atomic state distribution function (ASDF) is almost completely determined by electron excitation kinetics (EEK) whereas the plasma creation takes place due to the non-equilibrium state of the Saha balance of ionization and recombination /1/. To understand this mechanism we must study these equilibrium departures which due to the large electron density n_e may be small and difficult to find.

The zone of the plasma where the application takes place is mostly recombining. Here the deviations from equilibrium are more severe and attention must be paid to the role of molecules, atoms and radicals in the heavy particle excitation kinetics (HEK). To understand the applications of flowing plasmas not only insight in the flow magnitude but also its composition is needed. Due to HEK processes this may largely deviate from the equilibrium value.

This contribution is mainly devoted to the diagnostics of flowing plasmas as developed in our group at Eindhoven University. Two flowing thermal plasmas will be considered: the cascaded arc created magnetized expanding plasma (CACMEP) and the inductively coupled plasma (ICP). We confine ourselves to spectroscopic techniques divided in *passive* and *active* spectroscopy. For the latter we can distinguish between *global* and *specific* techniques.
Passive spectroscopy is non-intrusive in nature. The emission which escapes the plasma is collected and analyzed. With active spectroscopy we manipulate the plasma making use of an external source. This application can be either intrusive or non-intrusive. Examples of the latter are Thomson and Rayleigh scattering for which laser radiation is scattered by free (Thomson) or bound (Rayleigh) electrons providing insight in properties of the electrons (ions and atoms) without disturbing the relevant quantities. Examples of intrusive active spectroscopy are time-resolved Laser Induced Fluorescence (t-LIF) and the Power Interruption (PI) technique. In the case of t-LIF only one *specific* atomic or molecular transition is disturbed and followed in time. Due to the PI a *global* disturbance takes place. Both the t-LIF and the PI technique give insight in the plasma dynamics, e.g. the re-establishment of a disturbed quasi equilibrium situation. Combination of the results obtained from both passive and active (global and specific) spectroscopy gives insight in the state of equilibrium departure.

2. THE CHARACTERIZATION OF THE STATE OF EQUILIBRIUM DEPARTURE

An important aim of diagnostics is to determine the state of equilibrium departure of a specific plasma part. In that respect it is useful to distinguish between the non-equilibrium aspect of translation and excitation kinetics. The first category can be described by the parameter $\gamma = T_e/T_h$ in which T_e and T_h are the temperatures of the electrons and heavy particles, {e} and {h}. It is to be expected that the relation $\gamma > 1$ holds for active plasma zones. For the second category the equilibrium departure as induced by EEK will be expressed using the b-factors; $b(p) = \eta(p)/\eta^s(p)$ i.e. the ratio of the actual value and the Saha value

$$\eta^s(p) = \eta_e \eta_+ \frac{h^3}{(2\pi m_e kT_e)^{3/2}} \exp(I_p / kT_e) \quad (1)$$

of the density of the atomic state *p*. Here $\eta(p) = n(p)/g(p)$ is the density n(p) of atoms in level p per statistical weight g(p) (for the electrons $g_e = 2$), I_p the ionization energy whereas the other symbols have their usual meaning. The value b=1 is present for levels for which

$$A_p + e + (I_p) \overset{s}{\Longleftrightarrow} A_1^+ + e + e \quad (2)$$

the Saha balance of ionization (to the right) and three particle recombination (to the left) equilibrates. This easily holds for higher excited states which (if b=1) are said to be in pLSE /1/. The "p" of *partial* refers to the fact that it can be applicable to a part of the atomic system whereas the "L" of *local* reflects the possible spatial dependency. Since the balance is ruled by free electrons (a typical EEK process), $\eta^s(p)$ does not depend on T_h or γ (cf. /2/).

It is possible that the whole system is in pLSE whereas $\gamma \neq 1$. The opposite situation of translational equilibrium ($\gamma = 1$) and excitational non-equilibrium ($b(p) \neq 1$ for several p values) might also be found in a particular plasma (part).

Deviations from pLSE (i.e. $b \neq 1$) are related to the non-equilibrium state of the Saha balance, which can be created by transport of radiation and/or ions (and electrons).

1) Outward transport (i.e. escape) of radiation disturbs the Saha balance such that the lower levels $p < p_\alpha$ are pushed towards values $b(p) > 1$. The p_α is the boundary level for which transitions induced by electron impact and radiative decay are of equal importance /1/.

2) Transport of ions. In ionizing stationary plasmas the outward ion transport (efflux) is supported by a stepwise ionization flow over the system of excited levels. This is generated by an equilibrium departure of the ASDF $b(1)>b(2)>b(3)$ ... etc. which can be described analytically /1/ provided the escape of radiation can be neglected. The situation $b(1)<b(2)<b(3)$ supporting the influx of ions is found in recombining plasmas /1, 3/.

To obtain insight in the Saha-equilibrium departure, the actual ASDF and the equilibrium ASDF-value, (i.e. $\eta(p)$ and $\eta^s(p)$ for various levels) has to be determined. The first is done by performing absolute emission measurements (AEM), the second needs information on n_e and T_e, e.g. obtained by Thomson scattering.

In many studies on thermal plasma it is argued that there is no need for measuring the ASDF since n_e is large enough and the Griem criterion fulfilled. The levels are expected to be populated according to LTE. However, Griem's criterion is only related to the position of p_α which is connected to the influence of the escape of radiation. Since there are other departure mechanisms (e.g. ion influx/efflux) this condition, though needed, is in many cases

insufficient. We will consider conditions in which the Griem criterion is fulfilled but departures from pLSE (b-values) in the order of 10^4 are still present /4/.

3. COMBINED THOMSON-RAYLEIGH SCATTERING

Thomson scattering is the scattering of electromagnetic (EM) radiation by free (or loosely bound) electrons. It can be seen as a combination of two processes: the forced vibration of electrons absorbing the radiation and an emission by these oscillating charges. The emissivity of the (re)emission is determined by the absorption coefficient of the absorption process and thus proportional to $n_e\sigma$. The cross section σ for absorption is very small so that a laser is needed to create significant re-emission. The Doppler effect for the two processes can be combined and seen as creating a frequency shift $\Delta\omega = \mathbf{k}.\mathbf{v}$ proportional to the component of the particle velocity $\mathbf{v}$ in the direction of the scattering vector $\mathbf{k} = \mathbf{k}_s - \mathbf{k}_i$ where $\mathbf{k}_s$ and $\mathbf{k}_i$ are the wave vectors of the scattered and incident radiation. It can be shown that

- n_e can (after calibration) be determined from the total amount of scattered radiation and that
- the (Doppler) dispersion of the scattered radiation gives the electron velocity profile (i.e. T_e)
- provided k^{-1} is smaller than the Debye length λ_d.

If the latter condition is not fulfilled larger clumps of charges instead of electrons will act as scatter centra, the basis of the collective scattering technique /5/. For the determination of n_e this means that the parameter $\alpha = k\lambda_d$ should be small enough. In our cases $\alpha < 0.3$ so that only slight departures from the n_e-value can be expected for which corrections are possible.

A method related to Thomson scattering (TS) is Rayleigh scattering (RS) which is the scattering by bound electrons in atoms and ions. In our cases the ionization degree is sufficiently low so that we may neglect the contributions of the electrons bound in ions. Since the velocity of the atoms and the corresponding Doppler broadening is very small, we can easily distinguish between the T and R signal: there is a small R peak (giving the neutral density n_a) superimposed on broad T spectrum (n_e and T_e). Thus measuring two scattering phenomena in one set-up is relatively easy and convenient in studying plasmas since the three important plasma parameters n_e, T_e and n_a can be measured simultaneously and locally /6/.

The main components of the set-up are: a frequency doubled Nd:YAG laser (λ = 532 nm) as a source and as a detector: a polychromator for dispersion and a gated light amplifier (GLA) in combination with a photo diode array (PDA) to collect the scattered and wavelength selected photons. This GLA-PDA combination has a nearly single photon counting ability.

Figure 1 shows the CACMEP set-up. The plasma created in an cascaded arc expands supersonically in a low pressure (typically 40 Pa) vessel. With this set-up fast deposition of Si

and C (amorphous, graphite and diamond-like) can be obtained. Another application is the creation of a beam of H atoms and/or H^- ions bunched in a magnetic field.

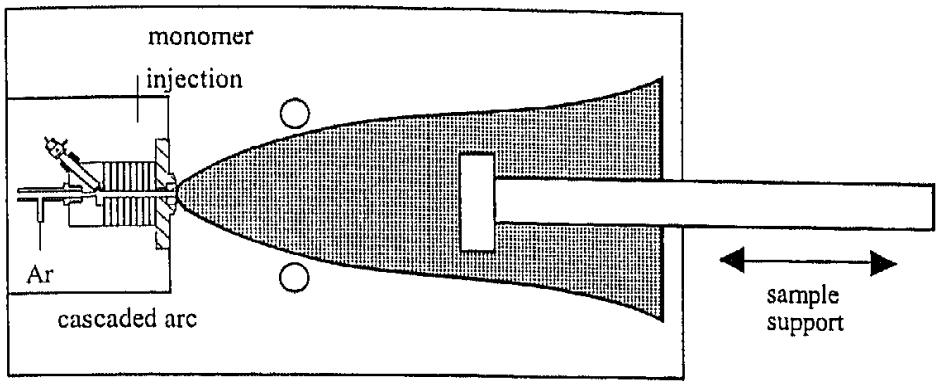

Fig. 1 The plasma supersonic expanding from a cascaded arc in a low pressure vessel

The Figs. (2a,b) give some results of the CACMEP. Figure 2a gives n_e as a function of the axial position for different percentages of hydrogen added to the main argon flow. The supersonic expansion and the stationary shock front can clearly be seen.

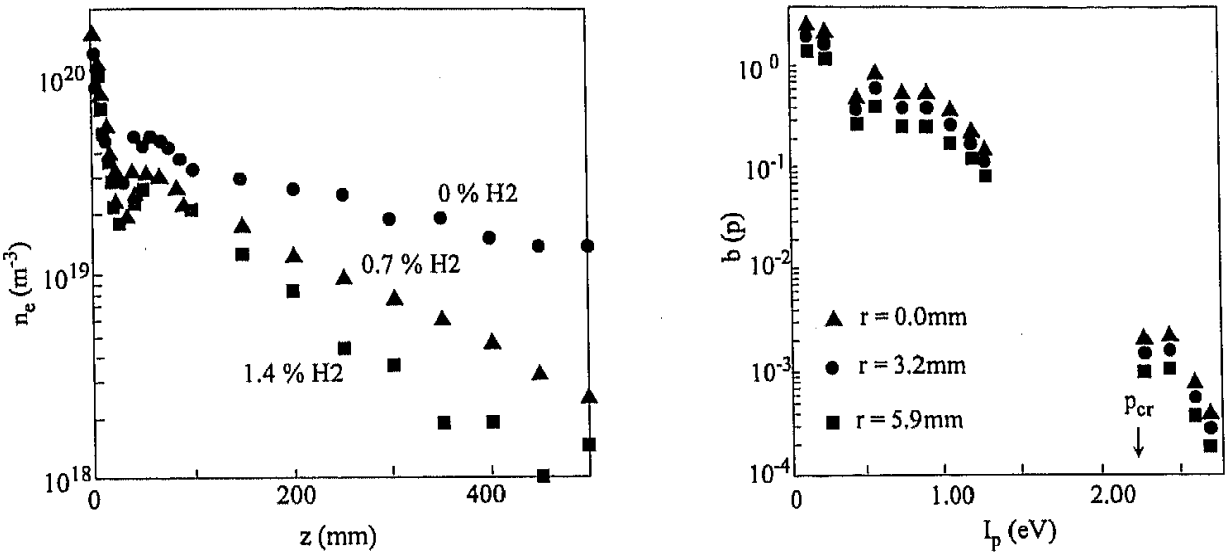

Fig.2 a) Results of Thomson scattering, n_e as a function of axial position for different percentages of hydrogen, I_{cas} = 45 A, Ar-flow = 3.5 slm, p = 40 Pa.
b) Combination of TS with AEM giving the $b (= n/n^i)$ -values for the pure Ar case as a function of the ionization potential I_p for z = 40 mm and four different radial positions.

If no hydrogen is present n_e remains relatively high whereas it decreases rapidly if hydrogen is present. The explanation for this observation is that H_2 in the vacuum vessel leads with Ar^+ to the formation of ArH^+ molecular ions. Subsequently dissociative recombination of ArH^+

molecules destroys the electron density. It is found that if other molecules are added we get a comparable chain of HEK processes: charge transfer followed by dissociative recombination. The n_e and T_e obtained from TS are used together with AEM to determine the b(p) as a function of ionization potential. The results of the pure Ar case (z = 40 mm) given in fig. 2b show that
- higher excited states are in pLSE, i.e. b=1 within the experimental uncertainties and that
- the equilibrium departure of lower states can be dramatically high (e.g. $b(4p) = 10^{-4}$),
- even though the condition $p>p_\alpha$ and thus the Griem criterion is fulfilled for almost any level.
The latter proves that the Griem criterion is not a sufficient criterion to guarantee the presence of pLSE for this case of the electron induced stepwise recombination flow.

4. TIME RESOLVED LASER INDUCED FLUORESCENCE

To get insight in the magnitude of the recombination flow we applied t-LIF on several Ar 4s - 4p transitions . Using a YAG-dye laser system tuned at the wavelength corresponding to the relevant 4s-4p transition, the 4p level density was enhanced by a factor of about 10^4. The decay of this population surplus after the laser pulse was found to be n_e dependent from which a total electronic destruction rate of $k(4p) \approx 2\ 10^{-13}\ m^3s^{-1}$ was deduced. This value was found to be much less than that predicted by /7/ but in good agreement with that postulated in /1/.

The t-LIF method is a powerful technique in the study of (de)excitation channels. For more information we refer to /8/ where, using t-LIF in a afterglow, a.o. the presence of Penning ionization channels have been demonstrated.

5. THE POWER INTERRUPTION TECHNIQUE

5.1 General. Thomson scattering was also performed on the inductively coupled plasma /9/. The obtained n_e and T_e in combination with AEM revealed that the ASDF of Ar in the ICP is much closer to pLSE than in the case of the CACMEP. To get insight in the more refined equilibrium departures the global active power interruption PI technique was used.
The essence of this technique /10-13/ can be understood from the stepwise nature of the energy balance of the steady state plasma showing that

$$EM \xrightarrow{Q} \{e\} \xrightarrow{Q} \{h\} \xrightarrow{Q} surr. \qquad (3)$$

- electrons {e} heated by the EM field transfer their energy to heavy particles {h}

- which happens predominantly in the skin via Ohmic heating (the two first links)
- implying that in this active zone the relation $T_e > T_h$ holds, whereas
- the last link, transport of {h}-energy towards surroundings, is mainly convective in nature.

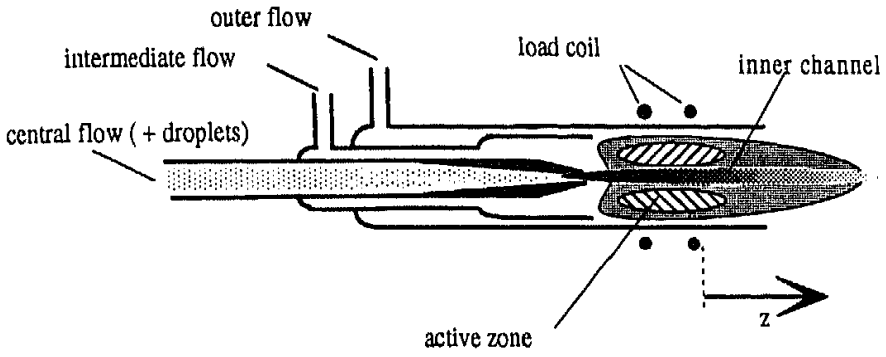

Fig.3 A schematic view of the ICP; the energy coupling EM→ {e} takes place into the skin from which heat is transported to the inner channel where the sample is injected.

Therefore the PI changes the local energy balance and alters the flow patterns giving:
- local and instantaneous responses, predominantly present in the skin and
-delayed responses related to the arrival of the flow disturbance.

The strength of the PI technique lies in the fact that the response times of the various processes are different: the time scales associated with the electron temperature relaxation equals $\tau_\varepsilon \approx 1\mu s$ that of the n_e relaxation $\tau_n \approx 100\mu s$, whereas the time of arrival $\tau_a \approx l/v$ depends on the velocity v and distance l traveled by the flow disturbance. This difference in relaxation times makes it possible to unravel the processes from eachother.

The experimental set-up is basically the same as that for absolute emission measurements. The pulses of the photo multiplier tube generated by wavelength selected photons are counted as a function of time by a multi channel scaler MCS . This MCS provides a series of 4096 time windows of 2μs each giving a record of 8ms. To obtain a good signal-to-noise ratio this procedure is repeated several thousand times.

In the following paragraphs we give brief descriptions of the experimental results. For more precise descriptions we refer to various detailed studies/9, 13-15/.

5.2 The delayed response gives rise to the ringing-like shape as given in fig.4 labelled with "5". By measuring the arrival time of this delayed response as a function of plasma position (i.e. after Abel inversion) insight can be obtained in flow patterns. It is found /13/ that
- the flow pattern is different for a dry (pure argon) and wet (argon + water) plasma,
- the plasma is accelerated in the load coil to a velocity of typically 12 m/s (P = 1kW) and that

- this velocity depends on the power since most of the power is converted into convective energy; i.e. $P \approx P_{conv} \approx 5/2$ vpA, with p the pressure and A the plasma cross section.

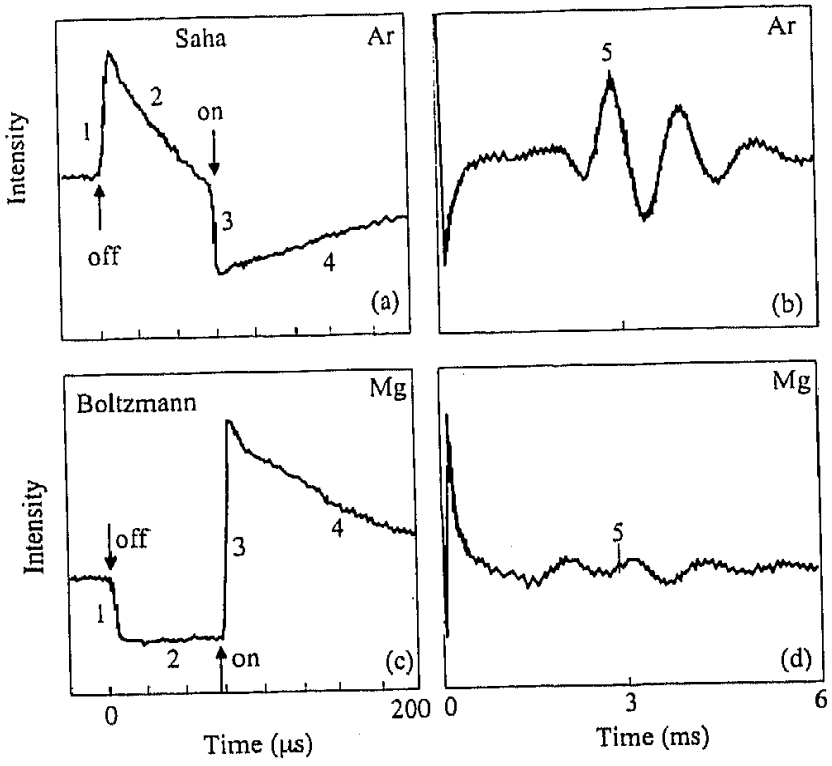

Fig.4 The instantaneous (left a+c) and delayed responses (right b+d) to the power interruption (between 0-75μs); the upper figures (a+b)refer to Ar 6p level, the lower (c+d) to MgI 3p.

5.3. The instantaneous responses predominantly present in the skin give, in contrast to flow-information-carrying delayed responses, insight in the excitation kinetics. If the power is switched-off the electrons will be cooled: $T_e \rightarrow T_e^* \approx T_h$, whereas the large particle reservoirs n_1, n_+ and n_e stay constant within τ_e. During this 'cooling' the system changes from ionizing to recombining after which n_e will decay as a result of recombination and diffusion. Re-switching the power gives 'heating' followed by 'ionization'. Therefore four events

1) cooling 2) decay 3) heating 4) ionization clearly separated in time can be distinguished.

5.3.1 The response to cooling is different for different atomic levels, not only in magnitude but also in sign. As an example the response of an Ar and a MgI line to the PI is shown in fig.4. The events: cooling (1), recombination (2), heating (3) and ionization (4) are depicted.

Note the opposite direction in the response to cooling (1) and heating (3) of the same line and the opposite nature of the response to cooling of Ar (fig. 4a) compared to that of MgI.(fig.4c). We say that the Ar line responds Saha-like and Mg Boltzmann-like.

5.3.2 The Saha-like response to cooling of the argon lines can be understood realizing that the Ar levels are close to the ion groundstate so that the Saha balance (cf. Eqn. 2) is not easily disturbed. This implies that the higher levels certainly are in pLSE, i.e. b(p) = 1. The Saha balance is established within some *ns* so that the change from $T_e \rightarrow T_h$ can be followed instantaneously. The change in the Saha density is obtained using Eqn. 1 for T_e and T_h, which gives for the ratio of densities before ($\eta^s(T_e)$) and after ($\eta^s(T_h)$) cooling.

$$\ln\{j^s(p)\} = 3/2 \ln\gamma + (\gamma - 1) I_p / kT_e \qquad (4)$$

Plotting the measured height of the cooling jump in Ar as a function of I_p (cf. fig. 5), should give a straight line from which T_e and T_h can be deduced.

The response of the lower Ar levels (e.g. the 4p levels) to cooling might deviate from the behavior as that predicted by the Saha equation (cf. Eqn. 4). This is due to the ionizing state of the system. Before the switch-off the lower levels are overpopulated with respect to Saha, e.g.

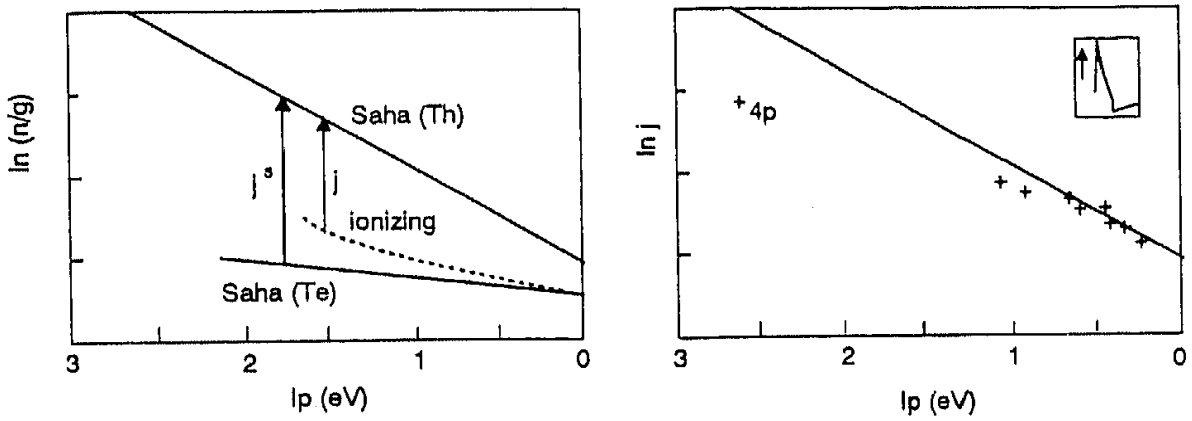

Fig. 5. The cooling jump of an ionizing system (dashed line) compared to that of full pLSE (solid) explains why the lower levels (e.g. Ar 4p) are below the line in 5b which plots the jump as a function of I_p

b(4p)>1, which is needed to create the stepwise ionization. If we assume that directly after the cooling the net ionization is quenched, and that the levels enter pLSE determined by $T_e^* = T_h$, we find for these levels the intensity jump ln[j(4p)] = ln[j^s (4p)] - ln[b(4p)] indicating that the higher b(4p) in steady state the lower the density jump will be (cf. fig. 5).

5.3.3 The decay of the argon lines in pLSE gives information on the decay of $n_e n(Ar_+) = n_e^2$ (cf. Eqn. 1). After Abel inversion by which the decay is obtained as a function of radial position, the steepest decay is found at the plasma edge. There the n_e decay is due to the outward diffusion. In the center of the plasma, recombination processes are more important.

The decay of hydrogen lines is found to be less steep than that of Ar lines and seems to be more or less synchronous to the decay of n_e. One should keep in mind that, since H is an addition and thus not the main supplier of atomic ions, the concentration $n(H_+)$ is not related to n_e. However, quasi neutrality demands that $n_e = n_+(Ar)$ so that Ar levels in pLSE depend on n_e^2.

5.3.4 The decay of continuum radiation. Fig. 6 gives a comparison between the response to a Saha line and the continuum. At cooling there is a jump downward instead of upwards as found for Saha dominated levels. The decay has a time-dependence which lies between that of the n_e and n_e^2 decay. The reason is that continuum radiation is composed of two contributions. One generated by electron-atom (e-a) interactions (with an $n_e n_a$ dependency) the other by electron ions (e-i) interactions ($n_e n_i = n_e^2$ dependent). The study of the decay of the continuum radiation as a function of time in comparison with the decay of argon lines makes it possible to unravel the e-i and e-a contributions from eachother. It is found /14/ that at moderate powers (below 1 kW) both contributions are of the same order of magnitude. For higher powers the e-i becomes dominant. This method can be used to find the ionization ratio n_e/n_a.

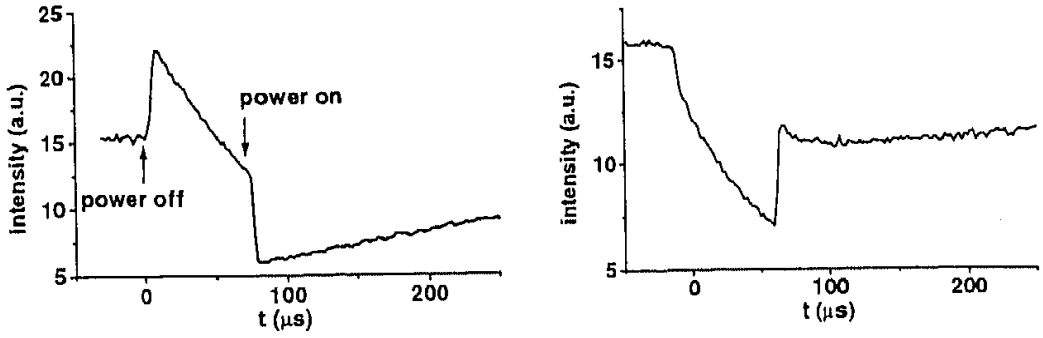

Fig. 6 The response of the continuum emission (right) compared to that of an Ar line, note the different cooling response. Comparison of the decay gives the continuum composition.

5.3.5 The response of the Boltzmann balance is found for levels of atoms introduced into the plasma via the evaporation of water droplets. As shown in fig. 4 they respond differently as the levels of the main gas Ar. The difference between the Boltzmann and Saha response to cooling can be understood by realizing that in contrast to the levels in pLSE which are *below* the main population reservoir n_+, the levels populated by the Boltzmann balance

$$A_1 + e + (E_{1p}) \overset{B}{\Longleftrightarrow} A_p + e \qquad (5)$$

of electron excitation and de-excitation are above the main reservoir (the atom groundstate) n_1. This means that the corresponding population being proportional to $\exp(-E/kT_e)$ will decrease as a result of the electron cooling $T_e \rightarrow T_h$.

In a study of the response of Li lines as a function of height, power and flow /15/ it is found that there is a large variety in responses to PI and that the "pure" B-like response as given in fig. 4c is only found in a limited range of plasma conditions. For instance fig.7 shows the various responses of the same Li levels to PI as a function of axial position showing that the typical B-like response presented upstream disappears downstream. This change can be related to the change on the n_+/n_1 along the central axis.

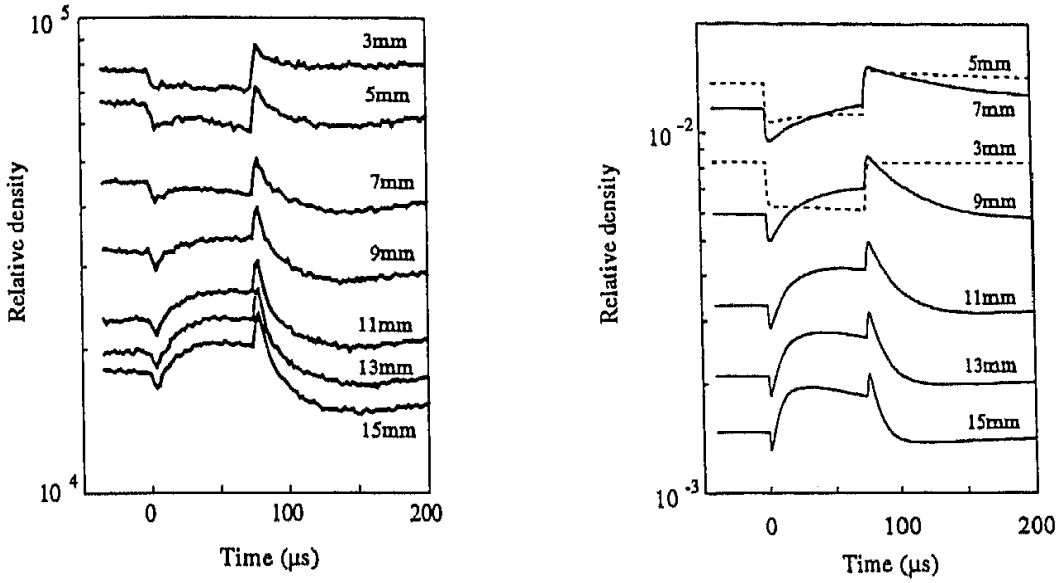

Fig.7. The measured and simulated responses of Li(2p) as a function of axial position.

1) At low n_+/n_1 values (for Li) found upstream the evaporation and ionization process is going on, which implies a creation and efflux of ions. Deviations from pLSE can be expected since the atomic system traveling along the temperature gradient ∇T_e is forced to adjust n_+/n_1, which initially will lack behind the value predicted by local Saha equilibrium LSE.

2) At $n_+/n_1 > 1$ more downstream we find that the initial downwards jump, the typical B-like response to cooling, is followed by an increase. This is based on the fact that cooling will effect the ratio n_+/n_1 as well. The Saha balances will be shifted in the recombination direction.

Since the shift to ionization degree reflected in the change of the responses of metal lines is largely determined by the temperature gradient ∇T_e and velocity v in the inner channel, the study of the responses to the PI provide insight in important transport parameters. The impact of the transport properties on the ASDF is studied /15/ constructing a collisional radiative model including transport phenomena. It is found that the simulation is successful in reproducing the observed responses as a function of axial position (cf fig 7).

5.3.6 Non-EEK processes are also unraveled by this technique. Typical HEK processes as charge and excitation transfer (CT and ET) are not sensitive to the electron cooling. Therefore their response to the PI must be different. It was found (cf. /13/) that the MgII level at (almost) the same total excitation energy as the ionization potential of Ar (15.8 eV) behaved differently. It was concluded that this was due to the influence of the CT reaction.

List of abbreviations

ASDF	atomic state distribution function	HEK	heavy particle excitation kin.
AEM	absolute emission measurements	ICP	inductively coupled plasma
CACMEP	cascaded arc created magnetized expanding plasma	pLSE	partial local Saha Equilibrium
		PI	power interruption
EEK	electron excitation kinetics	TR	Thomson Rayleigh

6. REFERENCES

/1/ J.A.M. van der Mullen, Physics report 191, 109 (1990).

/2/ J.A.M. van der Mullen, D.A. Benoy, F.H.A.G Fey, B. van der Sijde and J. Vlcek accepted for publication in Phys. Rev. E. (1994)

/3/ L.M. Biberman, V.S. Vorobev and I.T. Yakubov. "Kinetics of Nonequilibrium Low-Temperature Plasmas," Consultants Bureau, New York (1987).

/4/ D.A. Benoy, J.A.M. van der Mullen, M.C.M. van de Sanden, B. van der Sijde and D.C. Schram, J.Q.S.R.T. 49 (2), 129 (1993) accepted for publication

/5/ B.F.M. Pots, J.J.H. Coumans and D.C. Schram, Phys. Fluids 24(3), 517, (1981)

/6/ M.C.M. van de Sanden, J.M. de Regt, G.M. Janssen, D.C. Schram, J.A.M. van der Mullen, and B.van der Sijde, Rev. Sci. Instrum. 63, 3369 (1992)

/7/ L. Vriens and A.H.M. Smeets, Phys.Rev. A 22, 940 (1980)

/8/ S. De Benedictis and G. Dilecce, invited talk ESCAMPIG 94, to be published in "Plasma Sources Science & Technology"

/9/ J.M. de Regt, R.A.H. Engeln, F.P.J. de Groote, J.A.M. van der Mullen and D.C. Schram, accepted for publication in Rev. Sci Instrum. (1994)

/10/ D.B. Gurevich and I.V. Podmoshenskii, Opt. Spectrosc. 18, 319 (1963).

/11/ K.-P. Nick, J. Richter and V.Helbig J.Q.S.R.T. 32: p.1 (1984).

/12/ E.L. Bydder and G.P. Miller, Spectrochim. Acta 44: 165 (1989).

/13/ F.H.A.G. Fey, W.W. Stoffels, J.A.M. van der Mullen, B. van der Sijde and D.C. Schram, Spectrochim. Acta 46B: 885 (1991).

/14/ J.M. de Regt, J. van Dijk, J.A.M. van der Mullen and D.C. Schram accepted for publication in J.Phys.D (1994)

/15/ F.H.A.G. Fey, D.A. Benoy, M.E.H. van Dongen and J.A.M. van der Mullen, accepted for publication in Spectrochim. Acta (1994).